J Mater Sci (2007) 42:5068–5073
DOI 10.1007/s10853-006-0390-3

Single crystalline silicon carbide nanorods synthesized by hydrothermal method

L. Z. Pei · Y. H. Tang · X. Q. Zhao · Y. W. Chen

Received: 12 December 2005 / Accepted: 1 May 2006 / Published online: 22 February 2007

Abstract A new and simple hydrothermal process has been used to synthesize single crystalline silicon carbide nanorods. The synthesized silicon carbide nanorods have a length of about 1 μm and nearly same diameter of about 40 nm. We have observed that the nanorods possess a well-defined single crystalline structure with a thin layer of amorphous silica on the surface. The X-ray diffraction analysis demonstrates that the structure of silicon carbide nanorods is β-SiC. Raman shifts of the silicon carbide nanorods are discussed and the oxide-assisted growth mechanism is proposed to explain the formation and growth of silicon carbide nanorods.

Introduction

SiC nanostructure is an important class of heteronanostructures due to their mechanical, chemical, thermal and electronic properties [1, 2]. SiC nanowires, nanorods and nanotubes are several kinds of important SiC nanostructures in the present. As the important nanoscale forms, SiC nanostructures have attracted much attention in recent years can be prepared by several different routes, such as template method [3], metal vapor–liquid–solid (VLS) catalyst synthesis [4–6], chemical vapor deposition (CVD) method [7,8] since SiC nanorods were prepared by Dai et al. [9]. In particular, SiC nanorods have shown excellently mechanical and field emission properties significantly exceeding those of the bulk SiC nanocrystal and would be favorable for applications in high temperature, high power, high frequency and field emission nanoelectronic devices [5, 10]. SiC nanorods have been synthesized by different methods, such as a high temperature reaction of carbon nanotubes with SiH_4 or silicon compounds [9, 11, 12], or a carbonthermal reduction of silica xerogels containing carbon nanoparticles [13]. In these techniques, starting materials, used as sources of silicon and carbon, require a special preparation procedure. SiC nanorods have also been produced by hot-filament chemical vapor deposition or heat treatment of the porolysis of a polysilazane polymeric precursor [14, 15]. Although in the methods simple precursor materials were used, a significant amount of metallic particles have been used to catalyze the reaction. In addition, SiC nanorods have been obtained by a carbothermal reaction of SiO and Si at temperatures of higher than 1200 °C [16, 17]. However, the preparation temperature is high (higher than 1000 °C in general) and these methods make this approach quite complicated and expensive. Therefore, the low temperature growth of SiC nanorods and development of less expensive synthesis methods are of great interests for technological applications.

Hydrothermal method has shown the potential to synthesize one-dimensional nanoscale materials at low temperature, such as carbon nanotubes, ZnO nanorods and α-MoO_3 nanobelts et al. [18–22]. In our past research, self-assembled silicon nanotubes without

L. Z. Pei · Y. H. Tang (✉) · X. Q. Zhao · Y. W. Chen
College of Materials Science and Engineering, Hunan University, Changsha, Hunan 410082, P.R. China
e-mail: yhtang@hnu.cn

L. Z. Pei
School of Materials Science and Engineering, Anhui University of Technology, Maanshan 243002, P.R. China

metal catalysts have been synthesized by hydrothermal treatment of silicon monoxide [23]. In this letter, we report a new and simple route to synthesize single crystalline SiC nanorods by hydrothermal method at a relatively low temperature. The reaction products have been characterized by field emission scanning electron microscopy (FESEM), transmission electron microscopy (TEM), selected area electron diffraction (SAED), high-resolution transmission electron microscopy (HRTEM), energy dispersive X-ray spectrum (EDS), X-ray diffraction (XRD) and Raman spectroscopy.

Experiment

All the raw materials used in the experiment were purchased from Hefei Mingyu Science and Technology Lt. Co. and were used without further purification. 1 wt.% SiC (purity: ≥99.1%, average particle size: <50 nm) and SiO_2 (purity: ≥99.5%, particle size: 30 ± 5 nm) powders were mixed with 59.4 mL distilled water. The mass ratio of SiC and SiO_2 is 4:1. Then the mixture was put into the reaction kettle with a volume of 1000 mL under the atmosphere pressure. After the reaction kettle was sealed, it was then heated to 470 °C, 9.5 MPa of pressure in the reaction kettle, 100 r/min of the rotating speed for the stirrer equipped in the kettle and the temperature and pressure were maintained for 24 h. Then, the reaction kettle was cooled naturally. Finally, light grey aqueous solution with some suspension was collected after the experiment. The sample was firstly observed using a JEOL JSM-6700F FESEM. TEM and HRTEM samples were prepared by putting several drops of solution with suspension onto a standard copper grid with a carbon film and the observations were performed using a JEOL JEM-2010 transmission electron microscope with 1.9 Å point-to-point resolution operating with a 200-kV accelerating voltage with a GATAN digital photography system. Chemical analysis was performed with an energy dispersive X-ray spectrometer attached to the TEM. XRD patterns were carried out on a Siemens D5000 X-ray diffractometer equipped with a graphite monochromatized CuKα radiation (λ = 1.541 Å). The samples were scanned at a scanning rate of 0.02°/s in the 2θ range of 20–80°. Raman measurement was conducted using a Laboram-010 Raman laser spectrometer with a resolution of 2 cm^{-1}.

Results and discussion

SEM examinations reveal a large amount of SiC nanorods formed with straight structure and several dozens of nanometers in diameter as shown in Fig. 1(a). The straight nanorods were randomly oriented with a length about 1 μm. Different from the nanorods prepared by metal-catalyst vapor–liquid–solid (VLS) growth process [9, 15], no metal catalysts are found at the tips of the SiC nanorods. An amount of nanoscale particles with several hundreds of nanometers are also observed which possibly becoming the unreacted SiO_2 and formed graphite carbon particles according to the following XRD and Raman analyses. The TEM image (Fig. 1(b)) shows that the SiC nanorods are made of straight and smoothly parts and the diameter is about 40 nm. Some of the SiC nanorods exist in the form of bunches pointed by white arrow in Fig. 1(b) and the corresponding higher magnification TEM image is shown in Fig. 1(c). The higher magnification TEM image is essentially the same thing as Fig. 1(b). Some nanorod bunches aggregate together and this might be due to the aggregation of the nanosized SiC with high surface energy under hydrothermal conditions [24]. A SAED pattern (Fig. 1(d)) corresponding to Fig. 1(b) was recorded along the [110] zone axis revealing the single crystalline structure. The extra steaks (indicated with white arrow) are characteristics of twinning or stacking faults [9, 25]. Therefore, the SAED result shows that the nanorods consist of a single crystalline β-SiC structure with some stacking faults or twinning which is further testified by the following HRTEM and XRD results. The EDS spectrum (Fig. 2) only from the nanorods shows that the rods contain only C, Si and O further confirming that the nanorods are SiC nanorods with a significant amount of silicon oxide outer layer. A copper grid was used in the TEM study. Hence Cu peaks are observed from the spectrum. SiC nanorods terminate with the closed cap, as confirmed from the SEM, TEM and the following HRTEM observation.

Figure 3 is the HRTEM images of nanorod body and growth tip distinctly showing that the nanorods is a kind of single crystalline structure. The interplanar spacing of nanorods is determined to be 0.25 nm according to the HRTEM measurement and the following calculation by the software of Digital Micrograph (Gatan Inc., Pleasanton, CA) applied in the HRTEM, matching well with the {111} plane of β-SiC. The morphology and crystalline growth direction of the SiC nanorods are a little different from those synthesized by other methods [5, 22, 23, 26]. The HRTEM images show {111} lattice image of the SiC single crystalline structure along the nanorod axis. Therefore, the HRTEM images show that the core of the nanorods consists of crystalline β-SiC, whereas their surface is covered by a thin amorphous layer with

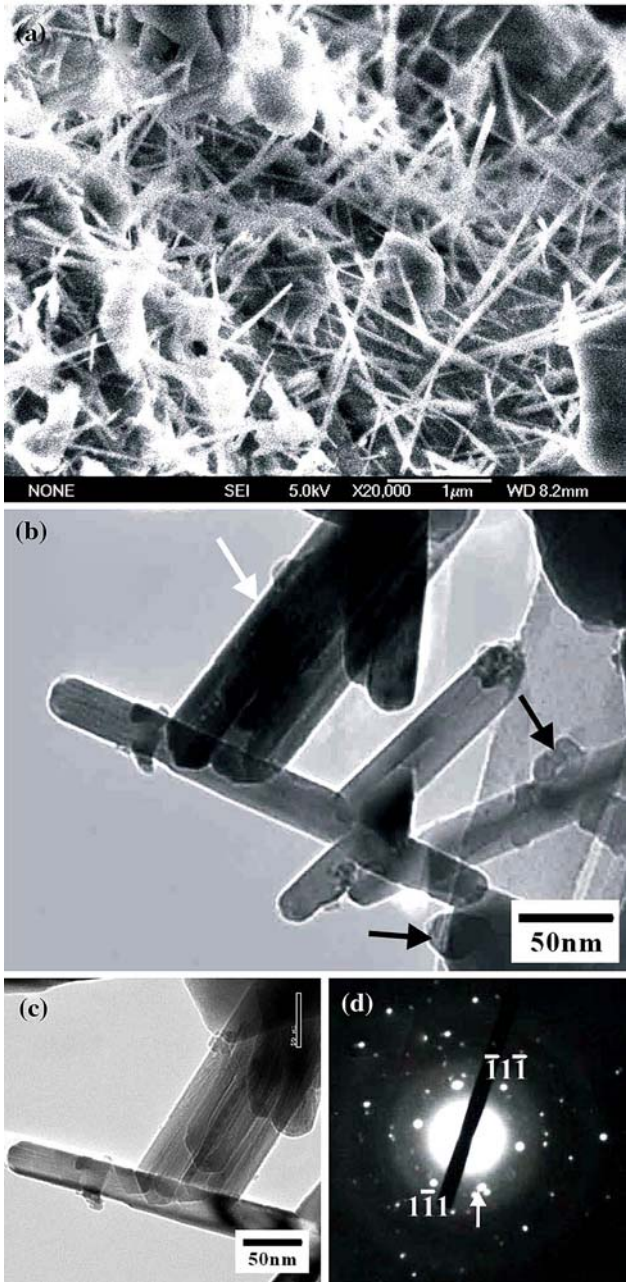

Fig. 1 SEM, TEM images and the corresponding SAED pattern of SiC nanorods. (**a**) SEM image of the SiC nanorods; (**b**) General TEM image of SiC nanorods. The nanoparticles are pointed by black arrow; (**c**) The TEM image of SiC nanorod bundles corresponding to the image pointed by white arrow in Fig. 1(b); (**d**) The corresponding SAED pattern indexed to SiC with extra streaks (indicated with an arrow) attributed to stacking faults or twinning showing the single crystalline structure

the thickness of less than 1 nm. Based on the EDS analysis (Fig. 2) indicating that our samples contain only silicon, carbon and a small quantity of oxygen besides the Cu peaks of Cu grids, we suggest that the surface layer of the nanorods is composed of SiO_2 [5].

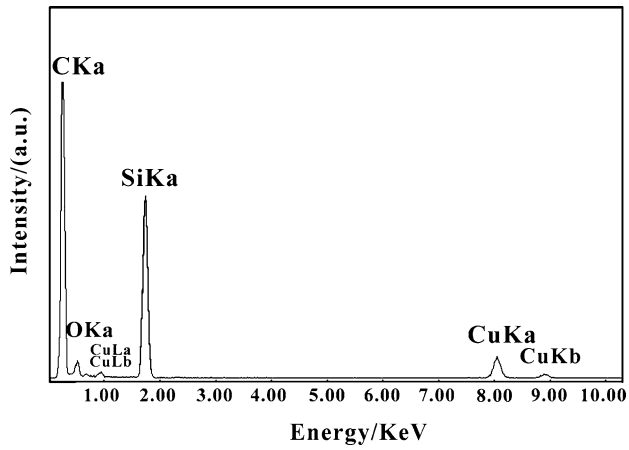

Fig. 2 EDS analysis of SiC nanorods

The growth tip of SiC nanorods can be clearly observed from the Fig. 3(b) further showing the nanorods have closed caps with very thin amorphous silica outer layers. The core-shell structure of the SiC nanorods is similar to that of the SiC nanorods grown by the hot filament CVD and carbonthermal reduction methods [13, 14].

The presence of the amorphous SiO_2 is also suggested by XRD analysis, showing a large peak centered at about 22° (pointed by black arrow in Fig. 4). In addition, the unreacted SiO_2 also contributes to the diffraction peak. Based on this result and taking account the used starting materials, we can suggest that the peak at about 22°, corresponding to amorphous phase in the XRD spectrum, can be attributed to the amorphous SiO_2. The XRD spectrum shown in Fig. 4 is characterized by intense peaks originating from β-SiC (JCPDS, No. 29-1129) and an amount of graphite carbon [27]. Therefore, we can conclude that the SiC nanorods have a β-SiC crystalline phase. Raman peaks in the region of 700–1000 cm^{-1} characterize the SiC species [26]. Bulk β-SiC crystalline with a zincblende structure has two Raman peaks in this region: transverse optical (TO) mode at 796 cm^{-1} and longitudinal optical (LO) mode at 972 cm^{-1}. The peaks at about 784.7 cm^{-1} and 915.1 cm^{-1} in the spectrum shown in Fig. 5 can be attributed to TO and LO modes, respectively. In this case the large red-shift of about 11.3 cm^{-1} for the TO mode and 56.9 cm^{-1} for the LO mode can be observed. The observed Raman shifts can be explained by taking into account the role of residual stress and quantum size confinement [17, 28, 29]. Raman peaks corresponding to the free carbon are observed in the region of 1300~1600 cm^{-1}. The graphite carbon signal is observed at the 1329.8 cm^{-1} and 1568.8 cm^{-1} corresponding to E_{2g},

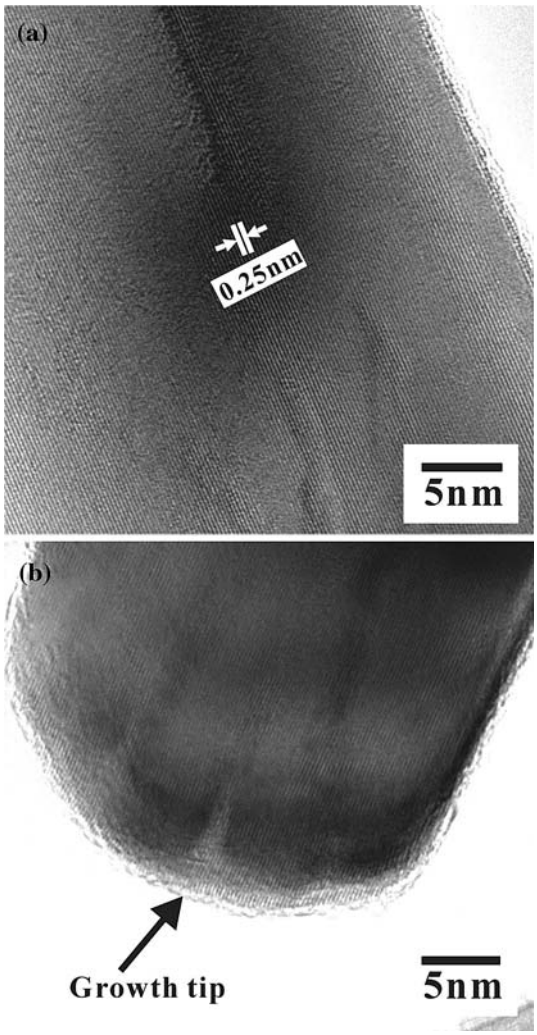

Fig. 3 Typical HRTEM images of SiC nanorods. (**a**) HRTEM image of the nanorod body; (**b**) HRTEM image showing the structure at the tip of the SiC nanorod

A_{1g} graphite modes [30] showing that the graphite carbon coexist in the SiC nanorod samples. The reaction kettle is composed of stainless steel (1Cr18Ni9Ti) and the carbon in the product may not have come from the kettle.

The core-shell structure of SiC nanorods is similar to that of Si nanowires with Si crystalline and silica shell synthesized by the oxide-assisted growth mechanism [31]. And we propose that the growth mechanism of SiC nanorods with core-shell structure can be explained by the oxide-assisted growth mechanism. There were no SiC nanorod structures detected by the TEM observation when the experiments were conducted in aqueous solutions with only SiC powders under the similar experimental conditions. Therefore, we propose that SiO_2 plays a very important effect on the nucleation and formation process of SiC nanorods.

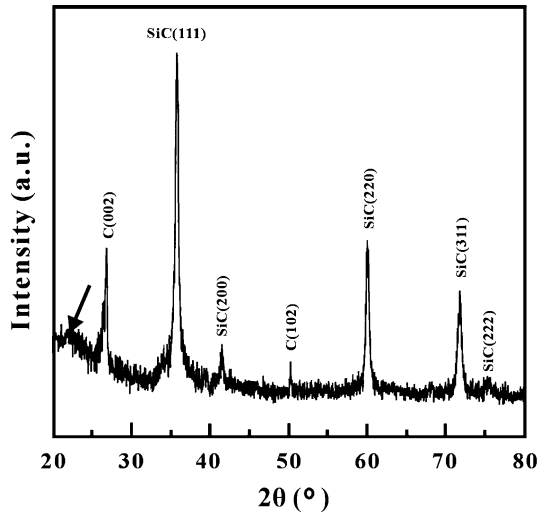

Fig. 4 XRD spectrum of the reaction product showing the β-SiC structure. An arrow indicates the amorphous phase corresponding to the thin silica outer layers of the SiC nanorods and unreacted silica

Water is almost absolutely vapored under supercritically hydrothermal conditions with high pressure. The melting point of SiC and SiO_2 becomes lower than the corresponding bulk materials and their reaction activity is higher because they are nanoscale particles in the course of high pressure. And supercritically hydrothermal conditions also accelerates the occurrence of some reactions. Hence the decomposition of SiC into Si and C and the reaction of SiC and SiO_2 may occur easily under supercritically hydrothermal conditions with high pressure [32–34]:

$$SiC \rightarrow Si + C \quad (1)$$

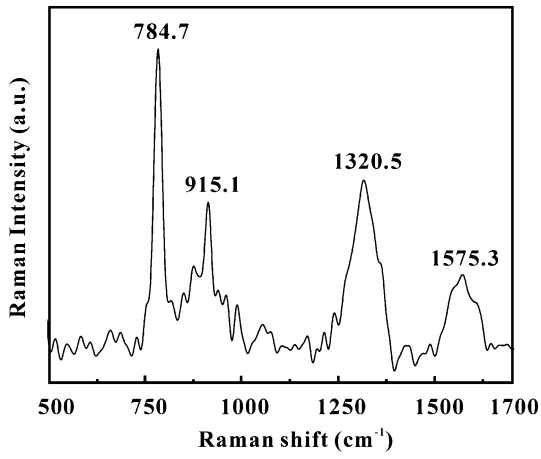

Fig. 5 Raman spectrum of the reaction product

$$2SiO_2(s) + SiC(s) \rightarrow 3SiO(g) + CO(g) \quad (2)$$

Therefore, the graphite carbon may form from the reaction Eq. 1. At the same time, the existence of some gas as a product in the reaction kettle when the temperature of the kettle is descended to the room temperature showing that CO gas possibly generates under supercritically hydrothermal conditions according to the reaction Eq. 2.

In our experiment, the low temperature rising occurs between 255 and 275 °C, keeping about 1 h and demonstrating that abundant heat can be absorbed. The phenomenon of the slow temperature rising between 255 and 275 °C is possibly due to the vaporization of water. A large amount of heat was absorbed during the vaporization process. After the most water is vaporized, the temperature rises again quickly. SiC nanoparticles can act as nuclei for the growth of SiC nanorods. But the ascending rate of temperature gradient of water with SiC and SiO_2 is lower than that of only water between 255 and 275 °C according to our experiment results when the volume of water and heating rate are same. So the nucleation process of SiC and SiO_2 possibly also occurs. Nucleation droplets larger than d_c will become stable nuclei, whereas droplets smaller than d_c will disappear gradually. The critical nucleus size can be expressed as [35]:

$$r* = (-2\gamma)/\Delta F_v \quad (3)$$

where γ is the specific interfacial free energy of the condensate-vapor interface and ΔF_v is the bulk free energy change per unit volume. We assume that the nanoscale particles and high pressure environment would increase interfacial free energy γ. Therefore, r^* becomes larger, which means that the droplets with larger diameters ($>r^*$) can grow to form SiC nanorods with thin silicon oxide outer layers. The oxide-assisted growth model of SiC nanorods is shown in Fig. 6. SiC core is coated by a small amount of silicon oxide outer layer resulting in the nucleation of SiC nanoclusters (Fig. 6(a)). And the SiC nuclei and nucleation nanoclusters will continue to grow following the deposition of the viscous silicon oxide at the growth tip of the nanorods under continual heating at high temperature and high pressure. In addition, the silicon oxide including SiO liquid layer assists the nanorod growth. The relatively thin silicon oxide on the nanorod tips plays the effect as a catalyst. Crystalline SiC stays inside the amorphous silicon oxide of nanorods under supercritically hydrothermal conditions. At the same time, silicon oxide continuously deposits in the surface

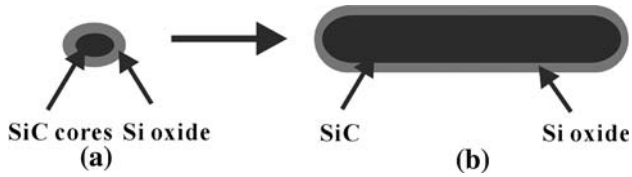

Fig. 6 The proposed oxide-assisted growth model of the SiC nanorods. (**a**) SiC nucleus with a small amount of silicon oxide outer layer; (**b**) SiC nanorods form by the oxide-assisted growth process

of SiC nanorods and results in the increase of thickness of silica sheath. The growth stage is assumed to involve that the relatively thin silicon oxide layer at the tip of nanorods forms a semi-liquid, which acts as a sink to absorb more silicon oxide. The stable silica restricts the non-one-dimensional growth of nanorods. However, the effect of silicon oxide at the tip of SiC nanorods is limited owing to only a small amount of silica absorbed from the environment resulting in the formation of the SiC nanorods with smooth surface (Fig. 6(b)).

Conclusions

In conclusion, a novel and simple hydrothermal method has been developed to synthesize single crystalline SiC nanorods with lengths in micrometers and diameters of about 35 nm. SEM, TEM, SAED, HRTEM and XRD analyses confirm that the nanorod is composed of a single crystalline β-SiC core with a very thin silica sheath with the thickness of less than 1 nm. The observed Raman shifts can be explained by taking into account the role of residual stress and quantum size confinement. The silica contributes to the growth of SiC nanorods and the oxide-assisted growth mechanism is proposed to explain the formation and growth of SiC nanorods. Compared with the other processes to synthesize SiC nanorods, the preparation temperature is relatively low and the hydrothermal method is simple and of low cost.

Acknowledgment This work was supported by the Doctoral Unit Funding of Educational Ministry under Grant No. 20040532014 and New Century Excellent Talent of Educational Ministry of PR China under Grant No. NCET-04-0773.

References

1. Rümmeli M, Borowiak-Palen E, Gemming T, Huczko A, Knupfer M, Cudzilo S, Kalenczuk RJ, Pichler T (2005) Synthetic Metal 153:349
2. Dong Y, Molian P (2003) Appl Phys A 77:839

3. Li YB, Xie SS, Zou XP, Tang DS, Liu ZQ, Zhou WY, Wang G. (2001) J Cryst Growth 223:125
4. Hu JQ, Lu QY, Tang KB, Deng B., Jiang RR, Qian YT, Yu WC, Zhou GE, Liu XM, Wu JX (2000) J Phys Chem B 104:5251
5. Choi HJ, Seong HK, Lee JC, Sung YM (2004) J Cryst Growth 269:472
6. Deng SZ, Wu ZS, Zhou J, Xu NS, Chen J (2002) Chem Phys Lett 356:511
7. Kang BC, Lee SB, Boo JH (2004) Thin Solid Films 464:215
8. Yang W, Araki H, Hu Q, Ishikawa N, Suzuki H, Noda T (2004) J Cryst Growth 264:278
9. Dai HJ, Wong EW, Lu YZ, Fan SS, Lieber CM (1995) Nature 375:796
10. Yang P, Yan H, Mao S, Russo R, Johnson J, Saykally R, Morrris N, Pham J, He R, Choi H (2002) Adv Func Mater 12:323
11. Han WQ, Fan SS, Li QQ, Liang WJ, Gu BL, Yu DP (1997) Chem Phys Lett 265:374
12. Mo YH, Shajahan MD, Lee YS, Hahn YB, Nahm KS (2004) Synthetic Metal 140:309
13. Meng GW, Zhang LD, Mo CM, Phillipp F, Qin Y, Li HJ, Feng SP, Zhang SY (1999) Mater Res Bull 34:783
14. Zhou XT, Wang N, Au FCK, Lai HL, Peng HY, Bello I, Lee CS, Lee ST (2000) Mater Sci Eng A 286:119
15. Yang WY, Miao HZ, Xie ZP, Zhang LG, An LN (2004) Chem Phys Lett 383:441
16. Gao YH, Bando Y, Kurashima K, Sato T (2001) Scripta Mater 44:1941
17. Kholmanov IN, Kharlamov A, Barborini E, Lenardi C, Bassi AL, Bottani CE, Ducati C, Maffi S, Kirillova NV, Milani P (2002) J Nanosci Nanotechno 2:1
18. Moreno JMC, Yoshimura M (2001) J Am Chem Soc 123:741
19. Wang WZ, Huang JY, Wang DZ, Ren ZF (2005) Carbon 43:1317
20. Liu B, Zeng HC (2003) J Am Chem Soc 125:4430
21. Wang JW, Li YD (2004) Mater Chem Phys 87:420
22. Wang ST, Zhang YG, Ma XC, Wang WZ, Li XB, Zhang ZD, Qian YT (2005) Solid State Commu 136:283
23. Chen YW, Tang YH, Pei LZ, Guo C (2005) Adv Mater 17:564
24. Yang RZ, Wang ZX, Dai L, Chen LQ (2005) Mater Chem Phys 93:149
25. Ho GW, Wong ASW, Kang DJ, Welland ME (2004) Nanotechnology 15:996
26. Nakashima S, Harima H (1997) Phys Status Solidi A 162:39
27. Jitianu A, Cacciaguerra T, Benoit R, Delpeux S, Béguin F, Bonnamy S (2004) Carbon 42:1147
28. Lu YM, Leu IC (2000) Thin Solid Films 377:389
29. Campbell IH, Fauchet PM (1986) Solid State Commun 58:739
30. Iijima S, Yudasaka M, Yamada R, Bandow S, Suenaga K, Kokai F, Takahashi K (1999) Chem Phys Lett 354:264
31. Wang N, Tang YH, Zhang YF, Lee CS, Lee ST (1998) Phys Rev B 58:R16024
32. Hähel A, Woltersdorf J (2004) Mater Chem Phys 83:380
33. Miller PD, Lee JG, Cutler IB (1979) J Am Ceram Soc 62:147
34. Santos WND, Baldo JB, Taylor R (2000) Mater Res Bull 35:2091
35. Chen YQ, Zhang K, Miao B, Wang B, Hou JG (2002) Chem Phys Lett 358:396